Int. J. Heat Mass Transfer. Vol. 28, No. 10, pp. 1859–1868, 1985
Printed in Great Britain

0017–9310/85 $3.00 + 0.00
Pergamon Press Ltd.

Mono-dimensional model analysis of solidification phenomena with subcooling using the enthalpy method

J. D. SAUZADE and J. GUION*

Laboratoire d'Ecothermique Solaire, CNRS, 06562 Valbonne, France and *Laboratoire de Chimie Physique, Université de Nice, 06034, Nice, France

(*Received* 30 *May* 1984)

Abstract—Performances of heat exchangers–accumulators working with phase-change materials (PCM) are limited by their discharge power. The purpose of our study is to outline the influence of crystalline kinetics and of subcooling on the recovery power of these accumulators. The behaviour of a layer of material with a PCM representative of salt hydrates, both taking into account, or not, the kinetics of crystal growth is investigated. Based on the enthalpy method, our model leads to the classical results related to the solidification of a substance having great chemical purity, and demonstrates the difference observed for technical materials, or mixed products, in purely thermodynamic conditions. Results are compared and analysed, using dimensionless numbers *Ste*, *Bi*, *Fo* and *Sol*, the 'solidification number' which is introduced in direct relationship to the kinetics of crystal growth. The model may be adapted, moreover, to crystallizations induced after subcooling; two examples of this process are given..

INTRODUCTION

STORAGE processing is fundamental for control and distribution of energy. Theoretical and practical studies concerning heat exchangers–accumulators working with liquid–solid phase change materials (PCM) have been performed for some years; these studies deal essentially with the low temperature storage process, and the appropriate PCM are paraffins and salt hydrates. The present work is mainly concerned with salt hydrates, but may be extended, with some precaution, to the paraffins.

The required qualities for a good storage material severely limit the number of PCM having industrial potential. To the main classical criteria for selection (high energetic density, chemical stability, melting temperature, etc.) must be added the need for strong kinetics of crystal growth. Our study makes possible the description of the solidification phenonema of a PCM by relating the kinetics of crystal growth to heat transfer. Its main interest lies in pointing out the role of subcooling phenomena and the associated consequences on the power values obtained during the discharge of such heat accumulators.

The aim proposed is to modelize the solidification of a layer of PCM, initially at a temperature equal to melting temperature, taking into account the kinetics of crystal growth, and the possible alteration of thermophysical properties, particularly the melting enthalpy, when technical PCM are used. The influence of impurities, whose presence may be desired for the modification of the PCM's properties [1–3], is clearly shown by a modification in the intrinsic enthalpy of the PCM, and by the need to introduce the notion of crystallizable fraction.

The aim of our modelization is to correlate the kinetics of crystal growth and the different aspects of solidification such as temperature profiles, extracted flux and the fraction crystallized, with time.

CRYSTALLIZATION MODEL WITHOUT CONSIDERATION OF THE KINETICS OF CRYSTAL GROWTH

We consider a PCM layer, initially at melting temperature, and in which only thickness e is finite. The upper limit is associated with an imposed temperature θ_∞, and the lower limit with an adiabatic condition $q_e = 0$ (Fig. 1). It is supposed that the convective heat transfer coefficient h is uniform and constant.

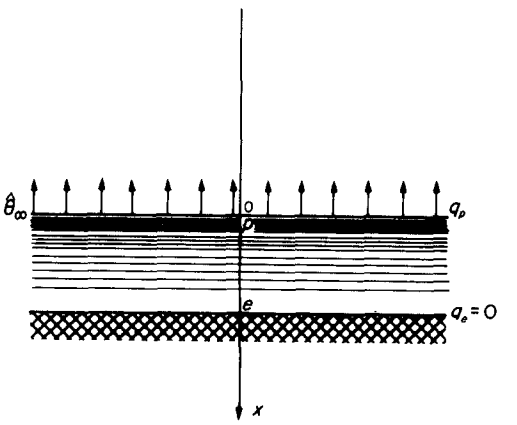

FIG. 1. Representation of PCM layer undergoing the phase change, with its limit conditions.

HMT 28:10-E

NOMENCLATURE

A	area of the surface from volume element V [m^2]
a	thermal diffusivity [m^2 s^{-1}]
b	$\sqrt{1-(\theta_f/\theta_f^*)}$
Bi	Biot number, he/k_s
c	concentration of saturated solution or specific heat
c_0	initial concentration of solution
c_0^*	concentration of 'ideal' material
$\hat{c}$	dimensionless specific heat, c_l^*/c_s^*
e	characteristic length, thickness of PCM layer [m]
F	crystallizable fraction
f	crystallized fraction
Fo	Fourier number, $k_s t/\rho c_s^* e^2$
ΔFo	dimensionless time step
h	convective heat transfer [W m^{-2} K^{-1}]
i	specific enthalpy [J kg^{-1}]
$\hat{i}$	dimensionless specific enthalpy
k_s	solid thermal conductivity [W m^{-1} K^{-1}]
k_l	liquid thermal conductivity [W m^{-1} K^{-1}]
$\hat{k}$	dimensionless thermal conductivity (liquid–solid), k_l/k_s
k	thermal conductivity, $Fk_s+(1-F)k_l$ [W m^{-1} K^{-1}]
$\tilde{k}$	dimensionless thermal conductivity, k/k_s
L^*	latent heat of solidification for ideal material
PCM	phase change material
q	surface heat flux [W m^{-2}]
$\hat{q}$	dimensionless surface heat flux
g	kinetic exponent
G	dimensionless kinetic coefficient
Sol	solidification number, $\tau_M \cdot k_s/\rho c_s^* e^2$
Ste	Stefan number, $c_s^*(\theta_f^*-\theta_\infty)/L^*$
t	time [s]
u	linear crystallization rate [m s^{-1}]
u_M	maximum linear crystallization rate [m s^{-1}]
V	control volume [m^3]
x	abscissa [m]
$\hat{x}$	reduced abscissa, x/e
X, Y, Z	control volume coordinates.

Greek symbols

θ	temperature [K]
$\hat{\theta}$	dimensionless temperature
$\hat{\theta}_f$	dimensionless melting temperature
$\hat{\theta}_M$	dimensionless temperature corresponding to $u = u_M$
$\hat{\theta}_i$	dimensionless initial temperature
θ_f	melting temperature of the PCM [K]
$\Delta\theta$	degree of subcooling, $\theta_f-\theta$ [K]
θ_f^*	melting temperature of 'ideal' material [K]
θ_∞	imposed cooling temperature [K]
ρ	volumic mass [kg m^{-3}]
τ	period of the crystallization phenomena, or characteristic time [s]
τ_M	maximal characteristic time [s]
$\hat{\tau}$	dimensionless characteristic time, τ/τ_M.

Superscripts

$\hat{}$	dimensionless
*	related to 'ideal' material.

Subscripts

f	fusion
l	liquid
M	maximal
p	wall
s	solid.

Enthalpy characteristic and crystallizable fraction

The presence of impurities in a PCM is generally associated with a decreased melting temperature and an enthalpy characteristic spread over a certain range of temperature (Fig. 2). Very important changes may be observed for a given PCM, according to the purity of this material. This explains the high dispersion of thermophysical values (enthalpy and melting point) reported in the literature for salt hydrates [4]. Moreover, technical materials always have a considerable content of impurities.

In order to take this into account, we consider the 'real' enthalpy characteristic of a PCM, and we define an 'ideal' PCM, hereafter associated with the symbol * (corresponding to at last 99% purity). If we consider the 'real' enthalpy characteristic, spread over a range of temperature, the degree of crystallization of PCM is related to the crystallizable fraction $F(\theta)$. This crystallizable fraction corresponds to the solid fraction deposited from the solution, at a given temperature, expressed from Raoult's law:

$$F(\theta) = \frac{c_0 - c(\theta)}{c_0^* - c(\theta)}. \quad (1)$$

If we assume that the shape of the liquidus, for the temperature range considered, is parabolic, $F(\theta)$ is expressed by

$$F(\theta) = 1-\left(\frac{\theta_f^*-\theta_f}{\theta_f^*-\theta}\right)^{1/2} = 1-b\left(1-\frac{\theta}{\theta_f^*}\right)^{-1/2}. \quad (2)$$

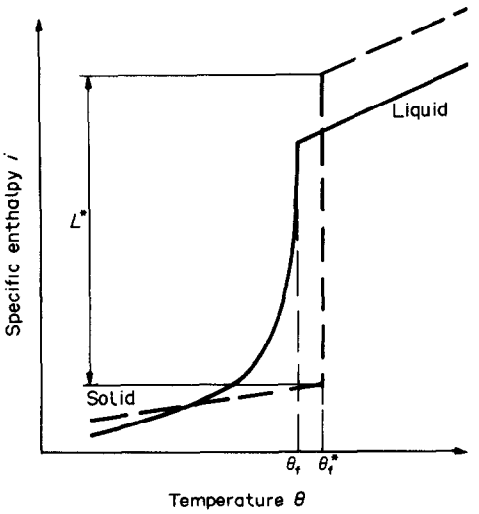

FIG. 2. Intrinsic enthalpy characteristics of a PCM as a function of temperature: --- 'ideal' behaviour; —— real behaviour (of the PCM).

Considering now an elementary volume V of PCM (Figure 3), for a temperature variation $d\theta$, the enthalpy variation related to mass unity, di, is

$$di = -L^* dF + Fc_s^* d\theta + (1-F)c_l^* d\theta \quad (3)$$

i.e. in expanding $F(\theta)$:

$$\frac{di}{d\theta} = L^* \frac{b}{2\theta_f^* \left(1-\frac{\theta}{\theta_f^*}\right)^{3/2}} - (c_l^* - c_s^*) \times \left[1 - \frac{b}{\left(1-\frac{\theta}{\theta_f^*}\right)^{1/2}}\right] + c_l^*. \quad (4)$$

By integration of equation (4), the analytic form of enthalpy i as a function of θ is obtained:

$$i(\theta) = bL^* \left(1-\frac{\theta}{\theta_f^*}\right)^{-1/2} + c_s^*\theta - 2b\theta_f^*(c_l^* - c_s^*) \times \left(1-\frac{\theta}{\theta_f^*}\right)^{1/2} + Cte. \quad (5)$$

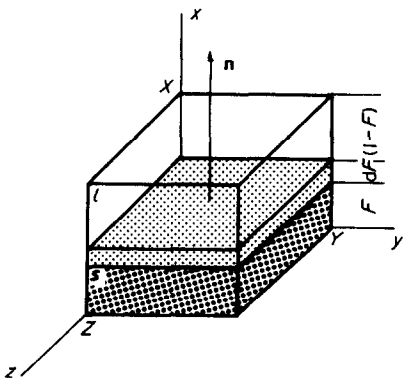

FIG. 3. Control volume for the mono-dimensional model proposed.

Enthalpy model analysis

The enthalpy model uses the heat conduction equation with non-linear coefficients and is easy to manipulate. Numerical methods are often the only way to find solutions to this equation. The use of apparent specific heat has been employed by some authors [5, 6]. In this case the latent heat of fusion is considered in a limited temperature interval close to the melting temperature θ_f [7–9]. In order to use the experimental results on enthalpy characteristics of PCM, $i(\theta)$, we kept the expression of the energy conservation in a control volume V (Fig. 3), in the following form:

$$\frac{\partial(\rho i)}{\partial t} = \text{div}\,(k\,\vec{\text{grad}}\,\theta). \quad (6)$$

Convection in the liquid phase, and dilatation phenomena related to volumic mass variations with temperature, are neglected.

Moreover, by using the notation of a crystallizable fraction, it is possible to formulate a law of thermal conductivity variation with temperature, which is written:

$$k(\theta) = F(\theta)k_s + [1-F(\theta)]\,k_l. \quad (7)$$

Our equations are then:

Energy conservation, equations (4) and (8):

$$\rho\frac{\partial i}{\partial t} = \frac{\partial}{\partial x}\left(k\frac{\partial\theta}{\partial x}\right). \quad (8)$$

Limit conditions:

$$k\left(\frac{\partial\theta}{\partial x}\right)_{x=0} = h(\theta_p - \theta_\infty) \quad \text{(third-order limit condition)} \quad (9)$$

$$\left(\frac{\partial\theta}{\partial x}\right)_{x=e} = 0 \quad \text{(adiabaticity limit condition)} \quad (10)$$

$$t = 0, \quad \theta(x,0) = \theta_f \quad \text{(initial condition)}. \quad (11)$$

Using equation (4), the enthalpy can be constantly related to the temperature θ, in the resolution of equation (8). We introduce the dimensionless variables defined by:

$$\hat\theta = \frac{\theta_f^* - \theta}{\theta_f^* - \theta_\infty}; \quad \hat x = \frac{x}{e}; \quad Fo = \frac{k_s t}{c_s^* \rho e^2} \quad (12)$$

$$\hat k = \frac{k_l}{k_s}; \quad \hat c = \frac{c_l^*}{c_s^*}; \quad \hat i = \frac{i(\theta_f) - i(\theta)}{L^*} \quad (13)$$

$$Bi = \frac{h\cdot e}{k_s}; \quad Ste = \frac{c_s^*(\theta_f^* - \theta_\infty)}{L^*}. \quad (14)$$

Equations (7)–(11) are rewritten in dimensionless notation:

$$\tilde k = \frac{k}{k_s} = \hat k + \left[1 - \left(\frac{\hat\theta_f}{\hat\theta}\right)^{1/2}\right](1-\hat k) \quad (15)$$

$$\partial\hat i = \partial Fo \cdot Ste \cdot \frac{\partial}{\partial\hat x}\left(\tilde k\frac{\partial\hat\theta}{\partial\hat x}\right) \quad (16)$$

$$\frac{\partial \hat{i}}{\partial \hat{\theta}} = \frac{1}{2}(\hat{\theta}_f)^{1/2}(\hat{\theta})^{-3/2} + (\hat{c}-1)Ste \cdot (\hat{\theta}_f)^{1/2} \cdot (\hat{\theta})^{-1/2} + Ste \quad (17)$$

$$\left(\frac{\partial \hat{\theta}}{\partial \hat{x}}\right)_{\hat{x}=0} = \frac{Bi}{\hat{k}} \cdot (\hat{\theta}_p - 1) \quad (18)$$

$$Fo = 0, \quad \hat{\theta} = \hat{\theta}_f. \quad (19)$$

This system of equations is solved with the help of an explicit scheme, using a physical approach. The model calculates the enthalpy content of every node at any given time. We then calculate the temperature of the nodes at a given time, by relation (17).

The enthalpy characteristic $i(\theta)$ being sufficiently spread, the attenuation of the crystallization front permits the use of an explicit scheme with no stability problem, and a mono-dimensional model is sufficiently simple to limit computing time.

However, several time steps have been tried; the value ΔFo is considered small enough when results between two consecutive cycles differ only by 10^{-3}. The space step is chosen arbitrarily as 0.1, so that a ΔFo value equal to 10^{-3} is satisfactory.

CRYSTALLIZATION MODEL WITH CONSIDERATION OF THE KINETICS OF CRYSTAL GROWTH

The modelization of heat accumulators working with PCM generally neglects subcooling effects, which are quite frequently observed with salt hydrates and even with organic materials. These phenomena have a primordial influence on the power obtained when discharging these accumulators.

Some authors [10] simulate the subcooling phenomenon in fixing arbitrarily a crystallization temperature different from the melting temperature, others such as de Jong and Bergmeijer [11] iterate on the value of the temperature to the point where the rates of propagation of the solidification front and that of linear crystallization agree. This method has the disadvantage of long computing times, and presents convergence difficulties during the iteration process. Moreover it can be used only if the enthalpy characteristic is sharply discontinued.

Our model reconciles both the enthalpy resolution method and the kinetics of crystal growth, but ignores inhibition phenomena linked to nucleation difficulties.

Numerous studies concerning crystal growing conditions have been performed, and different models related to salt hydrates developed [12–14]. From several experimental works [15, 16] it may be noted that the kinetics of crystal growth are characterized by two distinct steps:

—Initional growth phase, where the rate is expressed as

$$u(\theta) = C \cdot (\Delta\theta)^g \quad (20)$$

C being a constant, $\Delta\theta$ the degree of subcooling and g an exponent which can take values between 2 and 3.5. This initial step is governed by a thermodynamic driving force (free energy minimum principle), which increases with the degree of subcooling.

—For higher values of the degree of subcooling, the rate u decreases with increasing θ. This step is related to a high increase of viscosity [17], the consequence of which is limitation of the diffusion process at the liquid solid interface, and blocking of the kinetics of crystal growth decreases linearly with $\Delta\theta$ in the domain of temperature considered ($\Delta\theta \simeq 20°C$).

Expression of crystallized fraction when considering crystal growth kinetics

In the case where crystal growth kinetics are ignored. the enthalpy variation of a control volume V takes place at infinite rate, u_∞. Indeed, $F(\theta)$ and $i(\theta)$ characteristics correspond to equilibrium thermodynamic diagrams. Thus, any enthalpy variation with temperature must be reversible and be effected at a very slow rate, negligible compared to crystalline kinetics. $F(\theta)$ and $i(\theta)$ are state functions of the system, and depend solely on temperature; fraction $F(\theta)$ for a given temperature θ, corresponds to a maximum limit fraction for the PCM. This fraction is further designated as 'crystallizable fraction', and $i(\theta)$ as 'intrinsic enthalpy of the PCM'.

When we consider the influence of crystal growth kinetics, we associate with the control volume V, a crystallized fraction $f(\theta, t)$ which is no longer a state function, as it depends on time t. Knowledge of $f(\theta, t)$ is impossible; it is not a characteristic of a PCM. However, for a fixed temperature, we may know the evolution with time of the crystallized fraction of a control volume V. We call this crystallized fraction at constant temperature $f_\theta(t)$.

The solidification phenomenon may be considered from the point of view of formal kinetics as analogous to a first-order chemical reaction kinetic. At constant temperature, the crystallization process for a PCM 'M', may be written as:

$$\mathrm{M(l)} \underset{\theta,t}{\rightarrow} \mathrm{M(s)}. \quad (21)$$

For constant temperature, we thus write:

$$\frac{df}{f} = -\frac{1}{\tau(\theta)} \cdot t \quad (22)$$

where $\tau(\theta)$ represents the characteristic time or the period of the phenomena, with limit conditions:

$$\text{for } t = 0, \quad f_\theta(t) = 0 \quad (23)$$

$$\text{for } t \to \infty, \quad f_\theta(t) = F(\theta). \quad (24)$$

Integrating equation (22) and including limit conditions (23) and (24), we obtain the expression of crystallized fraction as a function of time, for the temperature θ:

$$f_\theta(t) = F(\theta)\left[1 - \exp\left(-\frac{1}{\tau(\theta)} \cdot t\right)\right]. \quad (25)$$

For a control volume V, if we consider a linear crystal growth rate in the x direction, the crystallized fraction is

$$f_\theta(t) = \frac{x}{X} \tag{26}$$

or

$$\left(\frac{\partial f}{\partial t}\right)_\theta \mathrm{d}t = \frac{\mathrm{d}x}{X} \tag{27}$$

that is

$$\left(\frac{\mathrm{d}x}{\mathrm{d}t}\right)_\theta = \left(\frac{\partial f}{\partial t}\right)_\theta \cdot X. \tag{28}$$

By derivation of equation (25) we obtain

$$\left(\frac{\partial f}{\partial t}\right)_\theta = \frac{F(\theta)}{\tau(\theta)} \cdot \exp\left[\frac{-1}{\tau(\theta)} \cdot t\right] \tag{29}$$

and substituting in (28)

$$\left(\frac{\mathrm{d}x}{\mathrm{d}t}\right)_\theta = \frac{F(\theta)}{\tau(\theta)} \cdot X \cdot \exp\left[\frac{-1}{\tau(\theta)} \cdot t\right]. \tag{30}$$

The linear crystal growth rate $u(\theta)$ is defined for a control volume where coordinate X is infinite. This corresponds to very small crystallized fractions, or in other words to very tiny time intervals, $t \to 0$. So we may write the relation between $u(\theta)$ and the period of the phenomena $\tau(\theta)$:

$$u(\theta) = \frac{F(\theta)}{\tau(\theta)} \cdot X. \tag{31}$$

Incremented and dimensionless writing of enthalpy and crystallized fraction variations

We consider the control volume V (Fig. 3), and we treat the crystallization process as a succession of an infinitely large number of isothermal crystallizations and cooling at constant crystallized fraction. For a crystallized fraction—always positive—equation (3) is rewritten:

$$\Delta i = L^* \Delta f_\theta(t) + c_s^* f(\theta, t) \Delta\theta + [1 - f(\theta, t)] c_l^* \Delta\theta. \tag{32}$$

Second-order terms $\Delta f(\theta, t) \cdot \Delta\theta$ have been omitted, and we find that for θ = constant we have by definition, $\Delta f(\theta, t) = \Delta f_\theta(t)$.

Following equations (25) and (29) we may write:

$$\Delta f_\theta(t) = \frac{F(\theta) - f_\theta(t)}{\tau(\theta)} \cdot \Delta t \tag{33}$$

Replacing $\Delta f_\theta(t)$ by its expression in (32) we get:

$$\Delta i = \frac{L^*}{\tau(\theta)} [F(\theta) - f(\theta, t)] \Delta t + f(\theta, t) c_s^* \Delta\theta + [1 - f(\theta, t)] c_l^* \Delta\theta. \tag{34}$$

We now introduce two new dimensionless parameters:

—A maximum characteristic time related to a segment of thickness Δx

$$\tau_M = \frac{\Delta x}{u_M}. \tag{35}$$

The dimensionless characteristic time will be in the form

$$\hat{\tau} = \frac{\tau}{\tau_M} \tag{36}$$

Thus, according to whether values of $\hat{\theta}$ are higher or lower than $\hat{\theta}_M$, the dimensionless temperature value for which the crystal growth rate is maximal (u_M), we have:

$$\hat{\theta} < \hat{\theta}_M; \quad \hat{\tau} = \mathscr{F}\left(\frac{\hat{\theta}_M}{\hat{\theta}}\right)^g \tag{37}$$

$$\hat{\theta} > \hat{\theta}_M; \quad \hat{\tau} = \mathscr{F}\left(\frac{G\hat{\theta}_M - 1}{G\hat{\theta} - 1}\right) \tag{38}$$

g and G being an exponent and a kinetic coefficient, respectively, obtained from studies of crystalization rate $u(\theta)$.

—A particular Fourier number which we designate for ease of discussion as *Sol*, the solidification number, defined as:

$$Sol = \frac{\tau_M \cdot a}{e^2}. \tag{39}$$

Equations (33) and (34) reformulated in dimensionless parameters become

$$\Delta f = \frac{\Delta Fo}{Sol \cdot \hat{\tau}} \left[1 - \left(\frac{\hat{\theta}_f}{\hat{\theta}}\right)^{1/2} - f\right] \tag{40}$$

$$\Delta \hat{i} = \Delta f + [\hat{c} - f(\hat{c} - 1)] \cdot Ste \cdot \Delta\hat{\theta}. \tag{41}$$

The system of equations (35)–(41) replaces equation (17), and permits the coupling of crystal growth kinetics with heat transfer equations. The computing process is identical with that presented in the first part of this paper and allows the determination of the temperature profile in the PCM layer at any time. To each time step value, the crystallized fraction is incremented by Δf, and the characteristic time $\hat{\tau}$ is computed, by equations (37) and (38). The convergence criterion is equivalent to that already mentioned, and the choice of $\Delta Fo = 10^{-3}$ is satisfactory.

RESULTS AND DISCUSSION

The above computing procedures lead to results particularly adapted to salt hydrates, considering the chosen domain for values of the different parameters:

dimensionless temperature, $\hat{\theta}_f$	0.1–0.001
Stefan number, *Ste*	0.2, 0.1, 0.05, 0.01
Biot number, *Bi*	1, 5, 10
solidification number, *Sol*	0.01, 0.1, 1.

Generally e is of the order of 1–5 cm [9, 10], and the value of $(\theta_f - \theta_\infty)$ is about 10°C.

The *Sol* and $\hat{\theta}_M$ parameters are connected to crystal growth rate. *Sol* reflects the maximum amplitude of crystal growth rate, $\hat{\theta}_M$ the phase displacement from θ_f^* in relation to the 'ideal' PCM of this amplitude. For example, for tetrahydrated calcium nitrate $Ca(NO_3)_2 \cdot 4\,H_2O$ we have, $Sol \simeq 0.01$ and $\hat{\theta}_M \simeq 1$ and for hexahydrated ferric chloride $FeCl_3 \cdot 6\,H_2O$ we have $Sol \simeq 0.2$ and $\hat{\theta}_M = 1.5$. The thermophysical properties of these two compounds are quite similar [4], but their crystal growth kinetics are very different.

Results obtained without taking crystal growth kinetics into account

Figure 4 stresses the importance of dimensionless melting temperature in crystallizable fraction values represented with relation to $\hat{\theta}$. Values of $\hat{\theta}_f$, given under each curve ($\hat{\theta}_f = 0.1, 0.05, 0.01, 0.001$) correspond to $\hat{\theta}$ values for $F(\hat{\theta}) = 0$.

It is seen that increasing $\hat{\theta}_f$ considerably diminishes the faculty of PCM crystallization. Even for low values of $\hat{\theta}_f$ (0.001) it seems impossible to recover all the latent heat of crystallization.

The determining influence of the $\hat{\theta}_f$ parameter is again shown in Fig. 5, enthalpy diagrams $\hat{i}$ as a function of $\hat{\theta}$. Biot and Stefan numbers being constant, the shape of the enthalpy characteristics $\hat{i}$ varies considerably if $\hat{\theta}_f$ varies. An increase of $\hat{\theta}_f$ for a given value of $\hat{\theta}$ gives rise to a large decrease in enthalpy content. As a correlation, the temperature domain where phase change occurs is notably enlarged.

It can be observed that for increasing values of $\hat{\theta}_f$, the PCM behaviour approaches that of a material with high specific sensitive heat.

If the $\hat{\theta}_f$ parameter acts directly on latent heat value ($\hat{i} = 1$ for $\hat{\theta}_f = 0$), the influence of variations of Stefan number acts on specific heat and thus on enthalpy. Figure 5 shows the mutual influence of $\hat{\theta}_f$ and *Ste*. For a

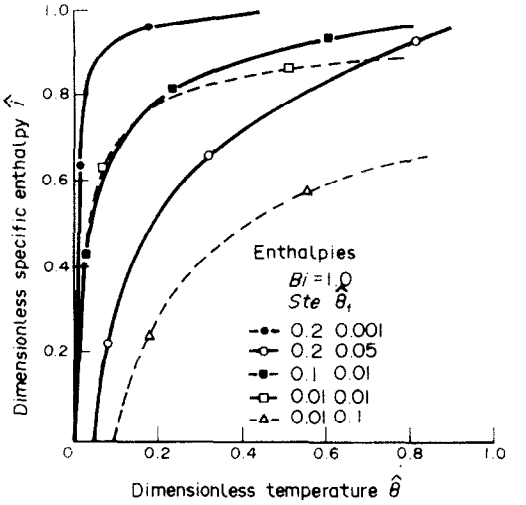

FIG. 5. Variation of enthalpy $\hat{i}$ with temperature; influence of Stefan number and $\hat{\theta}_f$ parameters.

same value of $\hat{\theta}_f = 0.01$ a higher value of *Ste* corresponds to a greater enthalpy content linked to a higher value of sensitive heat. It is also noted that for low values of *Ste*, in the solid state, the sensitive heat influence becomes negligible. This is shown for $Ste = 0.01$ by the similarity of the $\hat{i}(\theta)$ and $F(\hat{\theta})$ curves, indicating a negligible part of sensitive heat compared to latent heat L. Inversely for a fairly high Stefan number, $Ste = 0.2$, we note that the enthalpy content is greater than unity, from $\hat{\theta} = 0.5$, this being related to sensitive heat input.

Figure 6 illustrates the influence of $\hat{\theta}_f$ on the extracted flux $\hat{q}$ and the crystallized fraction. Heat flux extracted at cold surface is normalized to theoretical maximum value $h(\theta_f^* - \theta_\infty)$, so that:

$$\hat{q}_p = \frac{q_p}{h(\theta_f^* - \theta_\infty)} = \frac{\theta_p - \theta_\infty}{\theta_f^* - \theta_\infty} = 1 - \hat{\theta}_p. \qquad (42)$$

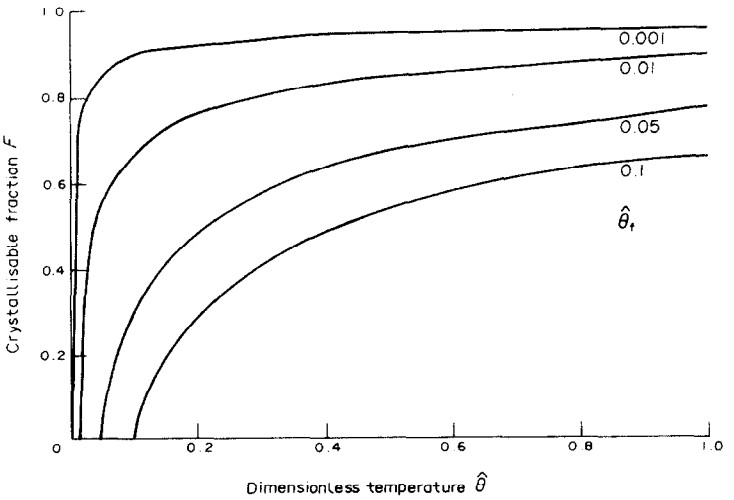

FIG. 4. Crystallizable fraction as a function of temperature, for different values of the $\hat{\theta}_f$ parameter.

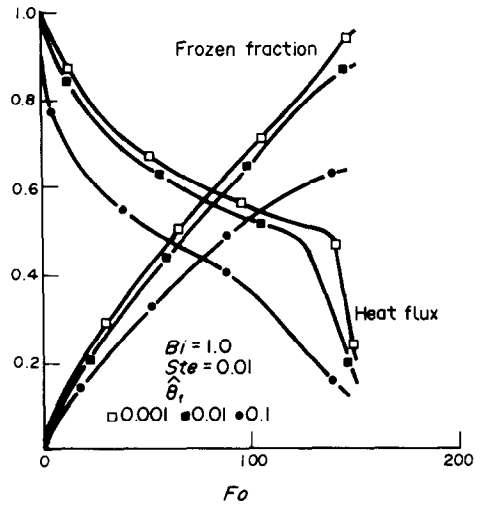

FIG. 6 Evolution (with time) of dimensionless flux and total crystallized fraction: influence of melting temperature $\hat{\theta}_f$.

In Figure 6 we see that the initial flux values are different for each $\hat{\theta}_f$ value because flux has been normalized in relation to the maximal theoretic value. For increasing $\hat{\theta}_f$ values, and with Biot and Stefan numbers constant, we note an important attenuation of the 'plateau', which is typical of extracted fluxes when a liquid–solid phase change occurs. It should be stressed that the advantage of PCM lies in the possibility of restoring latent crystallizing enthalpy with practically constant power. Figure 6 thus represents degradation of this aptitude with increasing values of $\hat{\theta}_f$.

Similarly, the crystallized fraction is weaker when $\hat{\theta}_f$ increases.

The influence of Biot number, shown in Fig. 7, which represents surface-extracted flux $\hat{q}_p$ and crystallized fraction, as functions of time Fourier number, is characteristic of the behaviour of PCM. As predicted, we observe attenuated variations of fluxes ('plateaux') on a broad time scale, only for low values of Biot number ($Bi = 1$). If we increase Bi, $\hat{\theta}_f$ and Ste being held constant, we observe a sudden lowering of $\hat{q}$ and a decrease in the length of the plateaux. The full exploitation of the advantages of plateau effects thus requires low values of Bi, compatible with the constraints imposed by the power necessary for the restitution of calories. A compromise between high values of $\hat{q}_p$ and their constancy with time may be established, considering that flux values are far from proportional to values.

In 'classical' models ($\hat{\theta}_f = 0$), the crystallized fraction is equal to unity when the flux plateau bends, indicating entry into the solid specific heat zone. In our case we observe only a change of curvature related to an increase in the crystallization fraction in this region.

Results obtained when taking crystal growth kinetics into account

We establish a distinction between results obtained during a normal crystallization, i.e. corresponding to spontaneous nucleation and crystallization without any experimental intervention, and induced crystallization, generally obtained by seeding a subcooled PCM, at a temperature θ_i, with the same material.

Normal crystallization. Figure 8 illustrates the evolution with time (Fo) of extracted fluxes $\hat{q}_p$ and the crystallized fraction. For values of $Bi = 1$, $Ste = 0.01$, $\hat{\theta}_f = 0.01$ and $\hat{\theta}_M = 1$, held constant, the various $\hat{q}_p$ profiles can be compared with the crystallized fractions, as a function of the solidification number Sol. Profiles are shown for different Sol, and on the same graph are the curves (broken lines) corresponding to $Sol = 0$, i.e. when crystal growth effects are ignored.

A high solidification number indicates slow crystal growth kinetics. It can be seen that extracted fluxes are greater when Sol values are low.

The flux profile for $Sol = 1$ is completely representa-

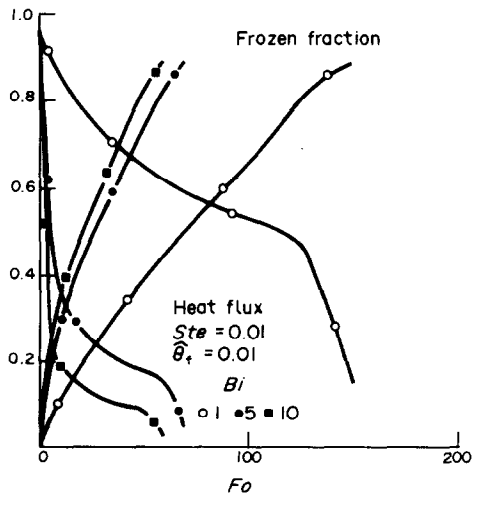

FIG. 7. Evolution (with time) of dimensionless flux and total crystallized fraction: influence of Biot number.

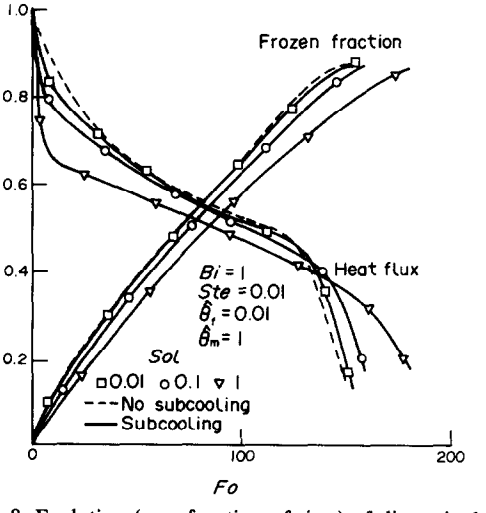

FIG. 8. Evolution (as a function of time) of dimensionless surface flux and total crystallized fraction, in presence of subcooling.

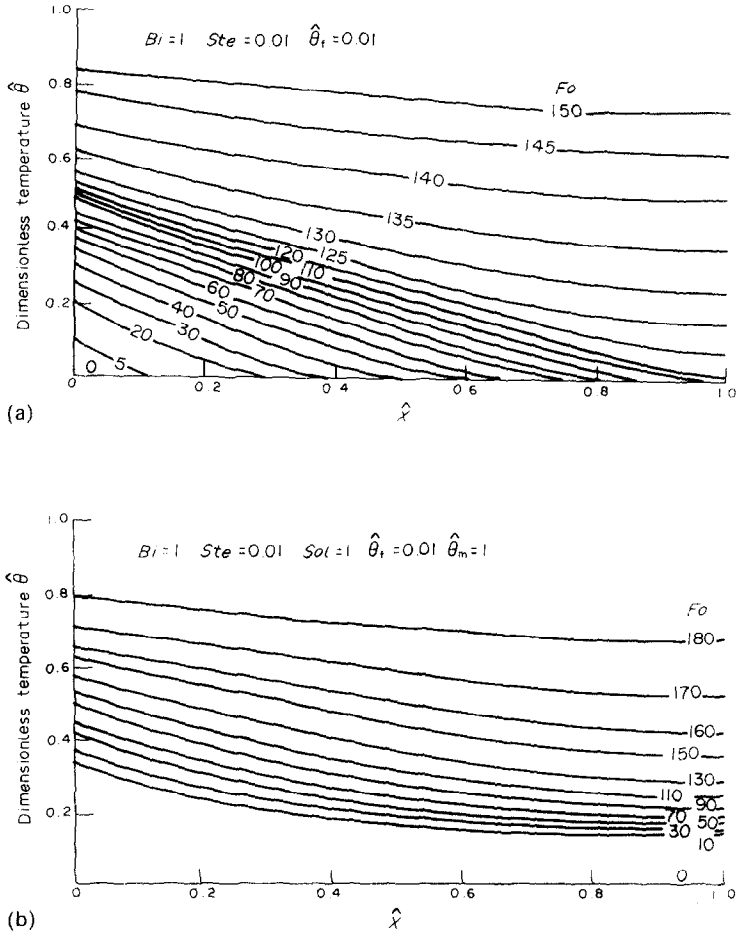

FIG. 9. (a) Distributions of dimensionless temperature, localization of melting front. (b) Distributions of dimensionless temperature, in presence of subcooling.

tive of a subcooling phenomenon. In comparison with the curve $Sol = 0$, the large initial decrease of $\hat{q}_p$ indicates a failure to crystallize, the flux being extracted by the sensitive heat of liquid PCM. The flux subsequently extracted along the plateau corresponds to a lower temperature level and to a region where crystal growth kinetics are low, which contributes both to a decrease in the efficiency of the extraction on one hand and to a decrease in the length of the plateau on the other.

We note also that crystallization is weaker when *Sol* values increase.

Figures 9(a) and (b) afford a comparison of the distribution of isotherms as a function of the dimensionless space parameter for different times characterized by one *Fo* value, when crystal growth kinetics are not or are included respectively, all the other parameters being equal.

In Fig. 9(a), neat characteristics obtained for $Ste = 0.01$, $Sol = 0.01$ and $\hat{\theta}_f = 0.01$ demonstrate the thermal behaviour of the PCM. Indeed, the crystallization is effected at $\hat{\theta}_f = 0.01$, which permits the solidification front to be localized precisely as a function of time (*Fo*) (for example: $\hat{x} = 0.1$ for $Fo = 5$). After some time ($Fo = 120$) isotherms are more spaced, indicating the end of solidification of the PCM.

In Fig. 9(b), we note that slowness of crystal growth ($Sol = 1$) is related to the complete disappearance of a crystallization front. The tardiness in crystallizing which is shown by a rapid decrease in temperature of the liquid PCM, in which heat is extracted out by sensitive heat, enlarges the temperature domain necessary to crystallization as far as $\hat{\theta}$ comprised between 0.15 and 0.25. The horizontal profile of isotherms outlines the low value of the extracted flux.

Induced crystallization. The model treats here the solidification of a PCM layer, maintained under subcooling, for an undetermined time. The initial crystallization temperature $\hat{\theta}_i$ is lower than melting temperature.

For fixed values of different parameters we have represented in Fig. 10, the flux variations $\hat{q}_p$ and crystallized fraction as a function of time (*Fo*). The broken curves relate to the case where there is no subcooling, i.e. $\hat{\theta}_i = \hat{\theta}_f = 0.01$.

We chose two values of $\hat{\theta}_i$ ($\hat{\theta}_i = 0.4$ and 0.6). The

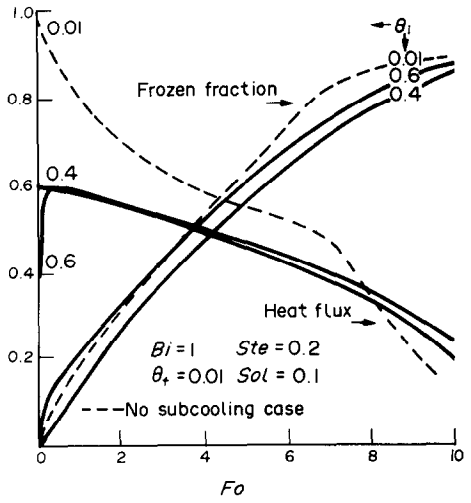

FIG. 10. Evolution (as a function of time) of dimensionless flux and crystallized fraction, in the case of induced crystallizations.

extracted flux value is seen to be much lower when crystallization is induced. In the case of $\hat{\theta}_i = 0.6$, the somewhat rapid initial increase is explained by strong kinetics of crystal growth at this temperature, the heat exchange explaining the decrease observed later.

There is also, for the two values $\hat{\theta}_i$, a notable increase in the length of the plateau. It is interesting to note that for $\hat{\theta}_i = 0.6$, the crystallized fraction is always greater than that for $\hat{\theta}_i = 0.4$, demonstrating that there is a compromise between crystallization process amplitude and heat transfer intensity.

In Fig. 11 we show the different enthalpic paths followed by the various nodes of the virtual network created in the PCM layer. The intrinsic characteristic enthalpy has been chosen for $Ste = 0.2$, a value high enough for the effects of sensitive heat in relation to latent heat to be observed. A value of $\hat{\theta}_i = 0.4$ has been chosen, the values of other fixed parameters being shown on the graph. We notice the enthalpy loss due to cooling with extraction of heat by liquid sensitive heat when there is subcooling. Node 1, the nearest to the flux extracting surface, is the most influenced by heat transfer. However, it can be seen that the enthalpic path is largely isothermic, reflecting the high crystal growth kinetics for this temperature. Nodes 5, 6, 8 and 11 show an almost instantaneous increase in temperature.

Moreover, we must stress that the linking of the different enthalpic paths with the intrinsic characteristic of PCM occurs without any instability of the model, even for low values of solidification number, for which the enthalpic paths are very close to the intrinsic enthalpy characteristic.

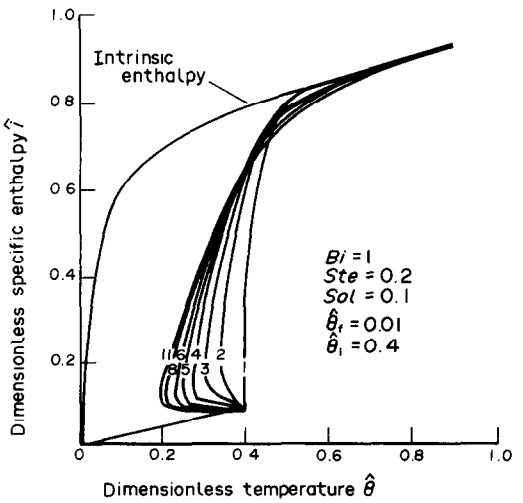

FIG. 11. Enthalpic paths for different nodes, in the case of induced crystallizations.

CONCLUSION

The model presented in this paper leads to a finer comprehension of solidification phenomena, in a heat exchanger–accumulator apparatus. Its use gives a truer understanding of the thermophysical behaviour of PCM and allows a reasonable estimation of power restored during discharge.

The mono-dimensional aspect of the model is not limitative, and the method may easily be extended to two- or three-dimensional models, if care is taken when defining the kinetics of crystal growth.

From a formal point of view, the same model may be used to describe the characteristic enthalpies of some organic materials, or even those of plastics. In this latter case, the model may help to simulate more precisely the cooling conditions which are important in the fabrication of these substances.

Acknowledgements—This paper has been sponsored by 'l'Agence Française pour la Maîtrise de l'Energie' (France).

REFERENCES

1. M. Laügt, J. D. Sauzade, S. Makhlouf, M. J. Wetterwald and J. Guion, Etude par microcalorimétrie différentielle d'hydrates salins, matériaux potentiels pour le stockage de l'énergie. *Calorimétrie et Analyse Thermique*, Vol. XIV. Journées de la Gaillarde (1983).
2. J. Sohns, B. Seifert and E. Hahne, The effect of impurities on the melting temperature and the heat of fusion of latent heat storage materials, *Int. J. Thermophys.* **2**, 71–87 (1981).
3. B. Carlson, H. Stymme and G. Wettermark, Storage of low temperature heat in salt hydrate melts calcium chloride hexahydrate. Report of Division of Physical Chemistry and Division of Building Technology, Royal Institute of Technology, Stockholm, Sweden (1978).
4. J. Guion, J. D. Sauzade and M. Laügt, Critical examination and experimental determination of melting enthalpies and entropies of salt hydrates, *Thermochimica Acta* **67**, 167–179 (1983).
5. P. H. Price and M. R. Stack, The effect of latent heat on numerical solutions of the heat flow equations, *Br. J. appl. Phys.* **5**, 285–287 (1954).
6. A. C. Cleland and R. L. Eule, The third kind boundary

conditions in numerical freezing calculations, *Int. J. Heat Mass Transfer* **20**, 1029–1034 (1977).
7. C. Bonacina, G. Comini, A. Fasano and M. Primicerio, On the estimation of thermophysical properties in non-linear heat conduction problems, *Int. J. Heat Mass Transfer* **17**, 861–867 (1974).
8. C. Bonacina and G. Comini, On the solution of non-linear heat conduction equations by numerical methods, *Int. J. Heat Mass Transfer* **16**, 581–589 (1973).
9. N. Shamsundar and E. M. Sparrow, Analysis of multi-dimensional conduction phase change via the enthalpy model, *J. Heat Transfer* **97**, 333–340 (1975).
10. D. Lecomte, Etude d'accumulateurs–échangeurs thermiques contenant des matériaux à changement de phase à basse température (20–80°C). Thèse Dr. Ingénieur, Ecole des Mines de Paris, Sophia-Antipolis, 06532 France (1983).
11. A. D. de Jong and P. W. Bergmeijer, Short term latent heat storage, *Energia Solare Nuove Prospettive, Atti della* 18[A] *Conferenza Internazionale*, Milano, Vol. 3, pp. 551–560 (1979).
12. J. W. Mullin, *Crystallisation*. Butterworths, London (1972).
13. R. F. Strickland-Constable, *Kinetics and Mechanism of Crystallisation*. Academic Press, New York (1975).
14. D. Elwell and J. H. Scheel, *Crystal Growth from High Temperature Solutions*. Academic Press, London (1975).
15. P. Pacak and H. Oesterreicherova, Crystal growth from concentrated aqueous solutions of calcium nitrate, *Crystal Res. Technol.* **16**, 1117–1121 (1981).
16. K. Gawron and J. Schröder, Properties of some salt hydrates for latent heat storage, *Energy Res.* **1**, 63–351 (1977).
17. C. A. Angell and R. D. Bressel, Fluidity and conductance in aqueous electrolyte solutions. An approach from the glassy state and high-concentration limit. I. $Ca(NO_3)_2$ solutions, *J. Phys. Chem.* **76**, 3244–3253 (1972).

MODELE MONODIMENSIONNEL A METHODE ENTHALPIQUE POUR L'ANALYSE DU PHENOMENE DE SOLIDIFICATION AVEC SURFUSION

Résumé—Les performances des échangeurs accumulateurs de chaleur travaillant avec des matériaux à changement de phase (PCM) sont limitées par leur puissance à la décharge. L'objet de l'étude est de souligner l'influence de la cinétique de croissance cristalline et de la surfusion sur la puissance de décharge de ces accumulateurs. Le comportement d'une couche de matériau PCM représentatif des hydrates salins est étudié en prenant en compte ou non la cinétique de croissance cristalline. Le modèle présenté utilise la méthode enthalpique, et conduit aux résultats classiques observés dans le cas de substances de grande pureté chimique ; il met en évidence les différences observées lorsqu'on utilise des produits techniques, où des mélanges, dans des conditions purement thermodynamiques.

Les résultats sont comparés et analysés à l'aide des nombres sans dimension *Ste*, *Bi*, *Fo* et *Sol*, 'nombre de solidification' qui est introduit en relation directe avec la cinétique de croissance cristalline. Le modèle peut être adapté aux cristallisations induites après surfusion ; deux exemples de ce processus sont examinés.

UNTERSUCHUNG VON ERSTARRUNGSPROZESSEN MIT UNTERKÜHLUNG MIT HILFE EINES EINDIMENSIONALEN MODELLS NACH DER ENTHALPIEMETHODE

Zusammenfassung—Die Leistungsfähigkeit von Regeneratoren, die eine Latentwärmespeichermasse (PCM) enthalten, ist durch die Entladeleistung begrenzt. Das Ziel unserer Untersuchung ist das Aufzeigen des Einflusses von Kristallisationsgeschwindigkeiten und der Unterkühlung auf die Entladeleistung dieser Wärmespeicher. Das Verhalten einer PCM-Schicht aus der Gruppe der Salzhydrate wird mit und ohne Berücksichtigung der Kristallisationsgeschwindigkeit untersucht. Auf der Grundlage der Enthalpiemethode liefert unser Modell die klassischen Ergebnisse bei der Erstarrung eines chemisch sehr reinen Materials und zeigt den beobachteten Unterschied zu technischen Substanzen oder Mischprodukten unter rein thermodynamischen Bedingungen. Die Ergebnisse werden verglichen und analysiert anhand der dimensionslosen Zahlen *Ste*, *Bi*, *Fo* und *Sol*, der "Erstarrungszahl", welche unter direktem Bezug auf die Kristallwachstumsgeschwindigkeit eingeführt wird. Das Modell kann darüber hinaus an die Kristallisationen, die nach einer Unterkühlung einsetzen, angepaßt werden ; zwei Beispiele zu diesem Vorgang werden angegeben.

ОДНОМЕРНЫЙ АНАЛИЗ ЯВЛЕНИЯ ОТВЕРДЕВАНИЯ ПРИ НЕДОГРЕВЕ, ПРОВОДИМЫЙ С ИСПОЛЬЗОВАНИЕМ МЕТОДА ЭНТАЛЬПИИ

Аннотация—Производительность теплообменников-аккумуляторов, работающих на материалах с фазовым переходом (МФП), ограничена их выходной мощностью. Цель исследования—описать влияние кинетики кристаллизации и недогрева на восстановительную способность аккумуляторов. Изучается поведение слоя материала с гидратами соли, взятыми в качестве МФП, как с учетом, так и без учета кинетики роста кристалла. Модель, основанная на методе энтальпии, приводит к классическим результатам, относящимся к отвердеванию химически высокочистого вещества, и демонстрирует отличие результатов, наблюдаемых для технических материалов или смешанных продуктов в чисто термодинамических условиях. Проводится анализ и сравнение результатов с использованием безразмерных числе *Ste*, *Bi*, *Fo* и *Sol*, 'числа отвердевания', которое введено в выражение для анализа кинетики роста кристалла. Модель может быть применена к процессам кристаллизации, возникающим в результате недогрева. Приведены два примера указанного процесса.